Available online at www.sciencedirect.com
SCIENCE DIRECT®
Talanta 60 (2003) 483–491
Talanta
www.elsevier.com/locate/talanta

Fluorescence analysis of the interaction of two peptide sequences of hepatitis GB virus C with liposomes

M. Muñoz [a,*], N. Rojo [b], I. Haro [b], V. Girona [a], C. Mestres [a], M.A. Busquets [a]

[a] *Physicochemical Department, Faculty of Pharmacy, Avgda Joan XXIII, s/n 08028 Barcelona, Spain*
[b] *Department of Peptide and Protein Chemistry, IIQAB-CSIC, Jordi Girona, 18-26, 08034 Barcelona, Spain*

Received 26 June 2002; received in revised form 15 November 2002; accepted 25 November 2002

Abstract

The physicochemical characterization of the peptide sequences E2 (39–53) and E2 (32–59) corresponding to the structural protein E2 of the GB virus C was done by studying their interaction with model membranes. The peptides showed surface activity concentration dependent when injected beneath a buffered solution. This tendency to accumulate into the air/water interface suggested a potential ability of these peptides to interact with bilayers. For that reason, Small Unilamellar Liposomes (SUVs) of 1,2-dimyiristoyl-sn-Glycero-3-Phosphocholine (DMPC) or 1,2-dimyiristoyl-sn-Glycero-3-[Phospho-rac-(1-glycerol)] (DMPG) were chosen as a mimetic membranes. A series of fluorescence experiments based on tryptophan peptide fluorescence or with fluorescence labeled SUVs, were done to cover different aspects of peptide interaction with bilayers. Steady state fluorescence anisotropy studies with *N*-(7-nitro-2-1,3-benzoxadiazol-4-yl) dioleoylphosphatidylethanolamine (NBD-PE) or 1-[4-(trimethylammonium) phenyl]-6-phenyl-1,3,5-hexatriene (TMA-DPH) labeled SUVs indicated that only the long peptide was able to change the lipid microenvironment of DMPG vesicles by slightly increasing the rigidity of the bilayer both above and under the lipid main transition temperature. These results were concordant with the slight blue shift of the maximum tryptophan wavelength emission after E2 (32–53) peptide incubation with DMPG vesicles. Our data provide useful information for the design of synthetic immunopeptides that can be incorporated into a liposomal system with a potential to promote a direct delivery of the membrane-incorporated immunogen to the immunocompetent cells, thus increasing the immuno response from the host.

Keywords: GB-virus C; Synthetic peptides; Fluorescence; Liposomes; Fluorescent probes

* Corresponding author. Tel.: +34-93-4024550/56; fax: +34-93-4035987.
E-mail address: mmunoz@farmacia.far.ub.es (M. Muñoz).

0039-9140/03/$ - see front matter © 2003 Elsevier Science B.V. All rights reserved.
doi:10.1016/S0039-9140(03)00079-1

1. Introduction

The synthesis and analysis of peptide segments of well characterized proteins has been widely used mainly to determine the role of each fragment on protein function and to extrapolate it to the physiological activity of the protein. For instance, the molecular details of membrane fusion have been stated with synthetic peptides corresponding to the putative fusion sequences of viral proteins as reviewed by Pécheur et al. [1]. Another example are the translocating peptides, sequences derived from the homeodomains of proteins acting as transcription factors involved in multiple morphological processes [2]. Among these peptides, pAntp was found to be responsible for the interaction of with DNA by binding specifically to cognate sites in the genome and, for the translocation of the entire homeodomain across cell membranes [3]. Another natural peptide fragment is *vasostatin-I*, derived from chromogranin A, a neuropeptide that has shown to kill a large variety of fungi and yeast cells [4]. Concerning to the immunological field, peptide-based vaccines present an advantageous alternative over traditional vaccine formulations specially if we consider production costs, high purity, defined structure and safety [5]. Thus synthetic peptides suppose a good approach to the design of well-defined synthetic immunogens capable of eliciting protective immunity against a disease. On the other hand, peptide fragments have been also useful to determine the common properties of a defined amino-acid sequence. For instance, the RGD sequence has been described to be of great importance as a universal recognition site [6].

Many of these studies have been done by analyzing the interaction of the peptides with model membranes, like lipid monolayers or liposomes combined with spectroscopic techniques. Particularly useful are the fluorescence experiments based on the intrinsic peptide fluorescence, due to the presence of tryptophan or tyrosine residues, or on extrinsic fluorescence by addition of external probes [2,7]. Fluorescence measurements give a great variety of information as peptide effect on binding behavior, lipid microviscosity, leakage, activity, structure or location of the peptides in the bilayers.

Considering the great potential of information derived from fluorescence studies, we have focussed our research in applying fluorescence techniques to the better understanding of GB virus C (GBV-C/HGV). The 5′ end of the GBV-C/HGV genome codes for the putative structural proteins C, E1 and E2, which appear to correspond probably (it is under debate) to components of the capsid protein and the virus envelope. Antibodies to the E2 protein of the virus occur after the loss of HGV-RNA in the serum and have been found in more than 5% of blood donors and in up to 30% of high risk groups.

In the present paper we describe a physicochemical study interaction of two peptide fragments with sequence E2 (39–53) GNVTLLCDCPNGPWV and E2 (32–53) GERVWDRGNVTLLCDCPNGPWV corresponding to the structural protein E2 of GB virus C based on the analysis of their interaction with lipid bilayers. The selected E2 peptide sequences are highly conserved among different isolates of GBV-C/HGV and also have conserved Asn-linked glycosylation sites. As described by Takahashi et al. [8] the selected region of E2 protein is most likely exposed on the virion surface and thus it can be recognised by neutralising antibodies. Peptides belonging to this E2 region could be useful to construct an antibody assay system to diagnose GBV-C/HGV infection. The main goal of our investigation was to study the influence of peptide length and amino acid sequence on the bilayer structure, in order to get insight into their role in protein recognition as well as their potential to be incorporated into antigen presenting systems like liposomes. Firstly, surface activity measurements were performed to test the ability of the peptides to accumulate into an air/water interface. Then, changes in peptide intrinsic Trp fluorescence in presence of SUVs and steady-state fluorescence anisotropy with labeled vesicles were done to cover different aspects of peptide–membrane interaction. Therefore, the results are discussed in relation to the contribution of the peptides to the depth of penetration into the membrane, lipid microviscosity alteration as well

Table 1
Primary sequence and isolectric point of E2 peptides

Peptide	Amino acid sequence[a]	pI
15-mer	GNVTLLC**D**CPNGPWV	3.80
22-mer	G**E**R**R**VW**D**R**R**GNVTLLC**D**CPNGPWV	4.56

[a] Positively charged amino acids at neutral pH are shown in bold; negatively charged amino acids at neutral pH are shown in bold and underlined.

as Trp localization in presence of zwitterionic or anionic membranes.

2. Experimental

2.1. Materials

1,2-Dimyiristoyl-sn-Glycero-3-Phosphocholine (DMPC), 1,2-dimyiristoyl-sn-Glycero-3-[Phospho-rac-(1-glycerol)] Sodium Salt (DMPG) were obtained from Avanti Polar Lipids (Birmingham, AL). *N*-(7-Nitro-2-1,3-benzoxadiazol-4-yl) dioleoylphosphatidylethanolamine (NBD-PE), and 1-[4-(trimethylammonium) phenyl]-6-phenyl-1,3,5-hexatriene (TMA-DPH) were from Molecular Probes (Eugene, OR).

2.2. Methods

2.2.1. Peptides synthesis

The E2 synthetic peptides reported in the present work belong to the N-terminal domain of the structural E2 protein of the virus and have the primary sequences and isolectric points indicated in Table 1. The syntheses were carried out on a Wang resin (0.72 meq g^{-1}) by a solid phase methodology following a Fmoc/tBut strategy by means of a *N*,*N*′diisopropylcarbo diimide (DIPCD)/1-hydroxybenzotriazole (HOBt) activation [9,10]. For difficult couplings, 2-(1*H*-benzotriazole-1-il)-1-3-3-tetramethyluroniumtetrafluoroborate (TBTU) and *N*,*N*-diisopropyl etilamine (DEIA) agents were used. Threefold molar excess of Fmoc-amino acids were used throughout the synthesis. The stepwise addition of each residue was assessed by the Kaiser's (ninhydrin) test [11]. Repeated couplings were carried out when a positive ninhydrin test was obtained. Different conditions were tested to cleave the peptide from the resin and to remove the side-chain protecting groups. Finally, peptide resins were treated with TFA solutions containing appropriate scavengers (either H_2O and ethanedithiol or H_2O, anisole and ethanedithiol).

Crude peptides were purified by preparative high performance liquid chromatography (HPLC) on a Shimadzu chromatograph equipped with a C8-silica column. The samples were eluted with a linear gradient of 60% H_2O (0.05% TFA)/40% acetonitrile (0.05% TFA) to 40% H_2O (0.05% TFA)/60% acetonitrile (0.05% TFA) in 30 min at a flow rate of 5 ml min^{-1} and detected at 220 nm. Purified 15- and 22-mer peptides were characterised by analytical HPLC, amino acid analysis and electrospray mass spectrometry Table 2.

2.2.2. Surface activity measurements

Surface activity measurements to determine the equilibrium spreading pressure of the peptides were recorded by using a Langmuir film balance KSV5000, equipped with a Wilhelmy platinum plate [12]. Increasing volumes of an aqueous concentrated solution of the peptides were injected beneath the surface of a cylindrical Teflon trough (70 ml of capacity) through a lateral whole. During the experiments, the subphase was continuously stirred (SBS Instruments, Spain). Surface pressure was recorded as function of time until a steady-state value of pressure was obtained.

2.2.3. Liposome preparation

Lipids from chloroform solutions were dried in a round bottom flask under vacuum and kept overnight into high vacuum to remove any residual solvent trace. For vesicles used in steady state fluorescence measurements, an appropriate mole fraction of probe (NBD-PE or TMA-DPH) was added to the chloroform solution before drying. The dried lipids were suspended with Tris 10 mM buffer solution at pH 7.3 obtaining Multilamellar liposomes (MLVs). Small unilamellar vesicles (SUVs) were prepared by bath sonication (Lab Supplies, Hickesville, NY; Model G112SPIT) of the MLV suspension. Sonication was carried out under a Nitrogen stream above the gel to liquid

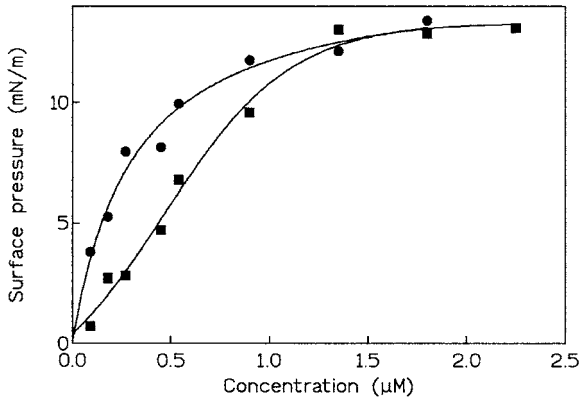

Fig. 1. Increases of surface pressure versus peptide concentration: ●, E2 (32–53); ■, E2 (39–53). Peptide was injected into a 10 mM Tris pH 7.4 subphase under constant stirring.

crystal transition temperature of the lipids. Liposome size was checked by dynamic light scattering (Malvern Autosizer) and was found to be 50 ± 0.2 nm with a polydispersity index about 0.1. Vesicles were used within 10 h. Final lipid concentration, assessed by phospholipid analysis [13], was 1.26 mM. Liposome suspensions were adjusted for spectrometric studies to 1 mM phospholipid.

2.2.4. Tryptophan fluorescence measurements

The fluorescence emission spectrum of Trp was monitored in Tris–HCl 10 mM, pH 7.8, and in presence of vesicles composed of either DMPC or DMPG. A 1-cm path length quartz cuvette that contained a final reaction volume of 2 ml was used in all experiments. Studies were performed on a SLM-Aminco, Series 2 Spectrofluorimeter, with excitation and emission wavelength set at 280 and 340 nm, respectively. A 4 nm slit was used for both excitation and emission. In these fluorimetric studies the lipid/peptide molar ratio was maintained high (100:4) so that the spectral contributions of free peptide would be negligible.

2.2.5. Steady-state fluorescence measurements

Steady-state fluorescence measurements were performed with the same spectrofluorimeter equipped with L-format fluorescence polarizers. The dynamics of lipids in SUVs were determined in presence and absence of peptides by measuring the depolarization degree of the fluorescence emitted form the probes NBD-PE or TMA-DPH. The excitation and emission wavelengths were set at 460/534 nm for NBD-PE and 365/425 nm for TMA-DPH. Anisotropy of SUVs labeled with 1% probe in absence (control) or presence of the peptide was automatically measured.

3. Results and discussion

3.1. Surface activity

The surface activity of both peptides was measured for concentrations ranging between 0.09 and 2.25 μM in a PBS subphase. Fig. 1, shows the pressure increases obtained in both cases. It can be seen that at low concentrations surface activity of E2 (32–53) is higher than for E2 (39–53). However, at high concentrations (> 0.9 μM) pressure increase is practically the same and both peptides reach a saturation in the surface activity at concentrations around 1.8 μM.

Table 2
E2 GBV-C peptides characterization

Peptide	Amino acid analysis[a]	HPLC[b]	HPLC/ES-MS
15-mer	D = 2.75(3); T = 0.69(1); *P* = 2.00(2); G = 2.22(2); V = 2.09(2) L = 1.93(2); C, W n.d.	$k' = 5.9$	$[M+H^+] = 1588$
22-mer	D = 4.66(4); T = 0.81(1) E = 0.95(1); P = 2.20(2) G = 3.37(3) V = 2.54(3); L = 2.07(2); R = 1.41(2); C, W n.d.	$k' = 3.6$	$[M+H^+] = 2486.04$

[a] Theoretical values in parenthesis.
[b] Eluents: water (0.05% TFA)/acetonitrile(0.05%). Flow: 1 ml min^{-1}. Detection: 215 and 280 nm.

Table 3
Values of excess and area/molecule

Concentration (μM)	E2 (39–53)		E2 (35–53)	
	Γ (mol m^{-2})	Area (nm^2)	Γ (mol m^{-2})	Area (nm^2)
0.09	3.16E−08	52.48	1.67E−07	9.94
0.18	1.29E−07	12.91	2.49E−07	6.66
0.27	1.40E−07	11.86	3.97E−07	4.19
0.45	2.50E−07	6.64	4.32E−07	3.84
0.54	3.69E−07	4.49	5.41E−07	3.07
0.9	5.60E−07	2.97	6.86E−07	2.42
1.35	8.07E−07	2.06	7.51E−07	2.21
1.80	8.32E−07	2.00	8.68E−07	1.91
2.25	8.79E−07	1.89		

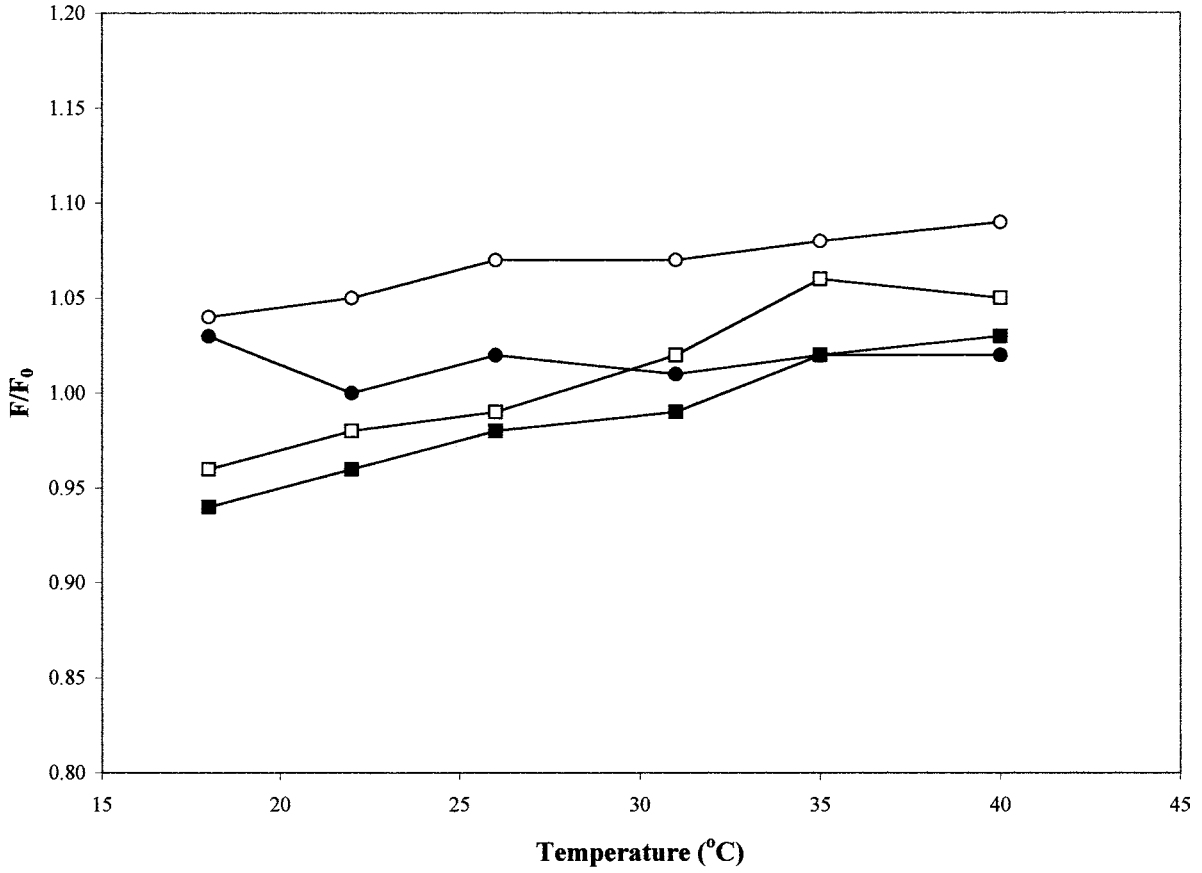

Fig. 2. Change in intrinsic fluorescence, expressed as F/F_0 where F denote the fluorescence intensity at 340 nm after and F_0, before the addition of SUVs to the peptide solution. E2 (35–53)/DMPC, ●; E2 (35–53)/DMPG, ○; E2 (39–53)/DMPC, ■; E2 (39–53)/DMPG, □. The lipid–peptide molar ratio was kept constant at 100:4 in all cases. Experiments were done in 10 mM Tris at pH 7.4. Error was with in 5%.

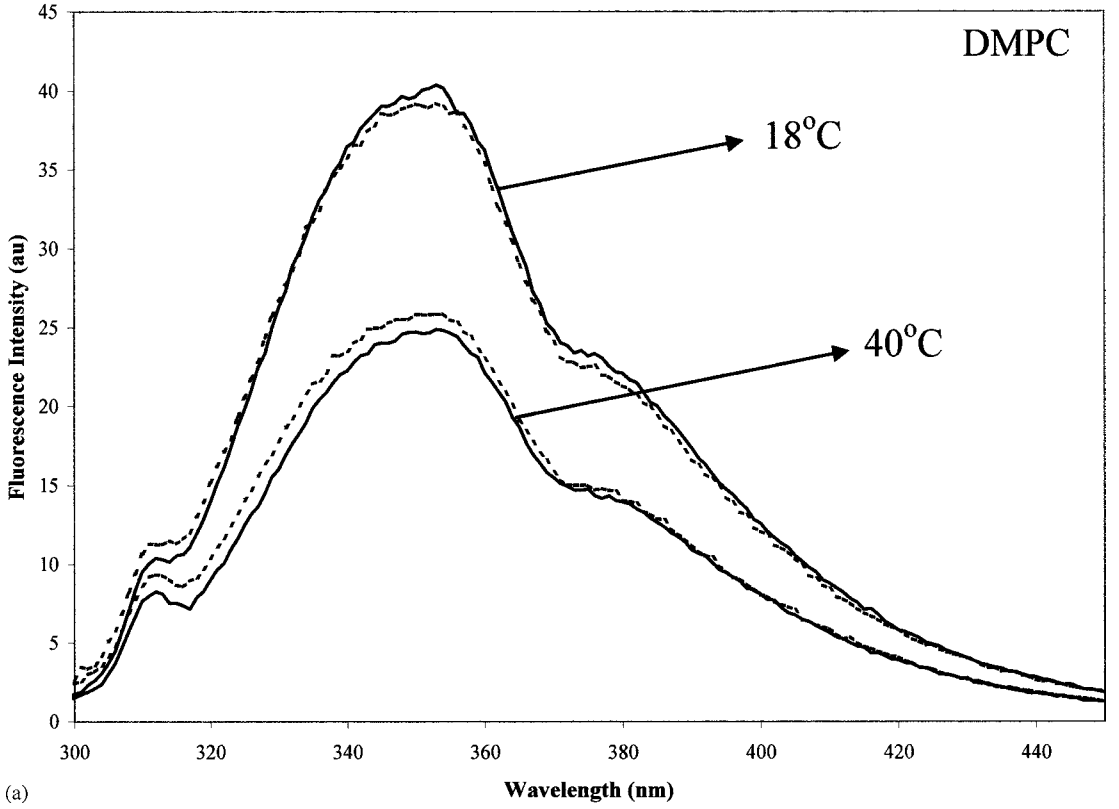

Fig. 3. Temperature dependence of Trp fluorescence of E2 (35–53) upon incubation with: (a) DMPC; or (b) DMPG SUVs. Solid line: peptide in solution; dotted line: peptide incubated with liposomes.

Surface activity was evaluated applying the Gibb's Equation (Eq. (1)) to calculate the surface excess to the curves where the equilibrium of $\Delta\pi$ versus time had already been determined.

$$\Gamma = \frac{1}{RT}\frac{\Delta\pi}{\Delta \ln c}, \quad (1)$$

where $R = 8.31$ J kmol^{-1}, $\Delta\pi$ is the pressure increase, T the temperature (294 K) and c the concentration of the peptide in the subphase. The area occupied by each molecule at the air/water interface was calculated using Eq. (2).

$$\text{Area} = \frac{1}{\Gamma N}, \quad (2)$$

where N is the Avogadro number.

The parameters obtained by the mathematical treatment of experimental data from surface activity curves are shown in Table 3. We can see more clearly that, at low concentrations, E2 (39–53) reaches in smaller amount the interface and consequently the area available for each molecule is higher. This behaviour could be explained by the smaller size of this peptide compared with E2 (32–53). The fact of being smaller could reduce the ability of the peptide to reach the interface. When the concentration increases it is possible that aggregates are formed that implies an increase in the size and then made the access to the interface easier. That could correlate with the fact that at high concentrations there is no difference in the activity of both peptides.

3.2. Tryptophan fluorescence measurements

The ability of the peptide to penetrate into a target membrane can be monitored as a function of the phospholipid composition of the bilayer by

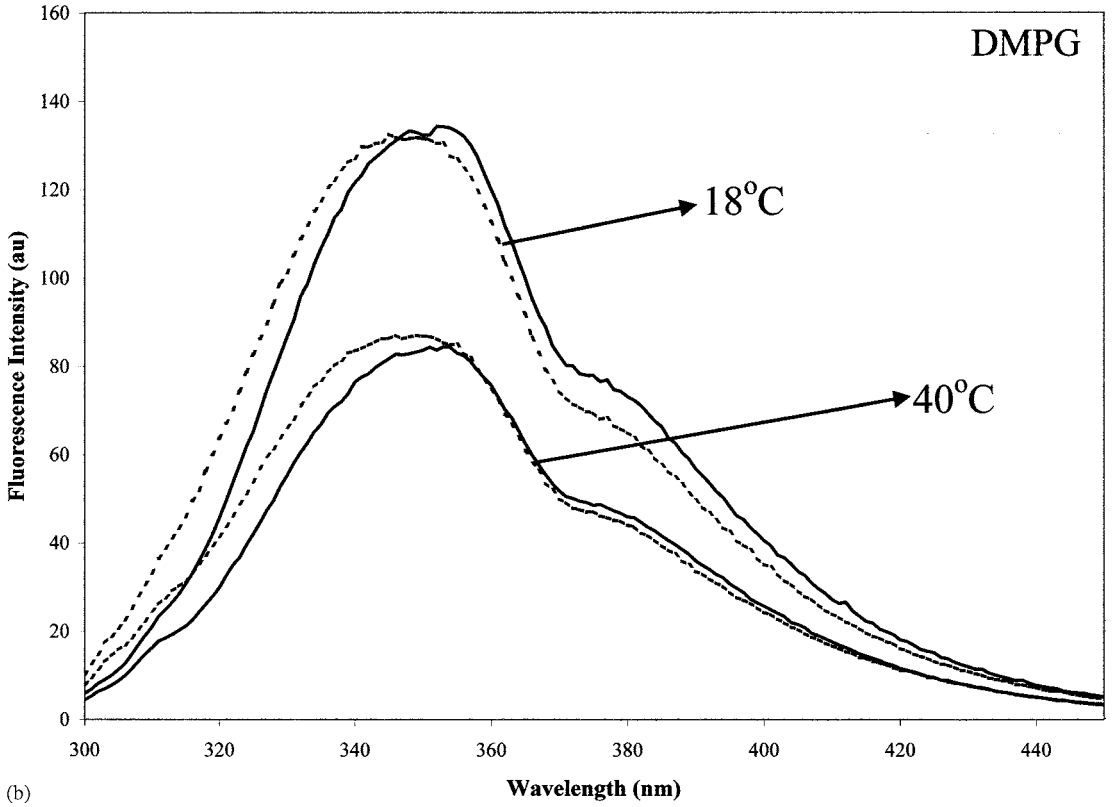

(b)

Fig. 3 (*Continued*)

following the changes in the intrinsic fluorescence of the Trp residue of the peptide. Fluorescence will increase when the amino acid senses a more hydrophobic environment, and in conjunction with an increase in quantum yield, the maximal spectral position will be shifted toward shorter wavelengths (blue shift). The maximum emission wavelength, λ_{max}, for Trp in solution in an aqueous environment is $\sim$353 nm. Spectra were recorded in the temperature interval between 18 and 40 °C, below and above, respectively, the phospholipid main transition temperature (Tm for DPMC and DPMG $\sim$23 °C). At 18 °C the acyl chains of the bilayer are rigid, in a gel state. On the contrary, at 40 °C, the bilayer is in a fluid state characterized by a higher acyl chain mobility. The results are discussed on basis to Trp λ_{max}, position as well as on the change in intrinsic fluorescence intensity, expressed as the ratio F/F_0, in absence and presence of liposomes. F and F_0 denote the fluorescence intensity at 340 nm after and before the addition of SUVs, respectively. F/F_0 has been described as the enhancement factor, ε, of the Trp fluorescence accompanying the binding of the peptide to the membrane [14].

λ_{max} of the short peptide, E2 (39–53), did not change upon incubation with SUVs at any of the tested compositions and temperatures. This means that Trp remains in an exposed environment [7], does not penetrate into the bilayer and consequently one could think about a lack of peptide binding. However, the ratio F/F_0 increases almost linearly with temperature and following a similar trend for DMPG and DMPC samples (Fig. 2) as if the Trp had restricted mobility due to relocation into the bilayer. It could be that the hydrophobic part of the peptide intercalates into the bilayer, as confirmed in lipid monolayer penetration kinetics (data not shown), while the Trp residue remains exposed thus indicating a weak surface interaction.

Table 4
Changes in intrinsic Trp Fluorescence upon E2 (32–53) incubation with DMPG vesicles as a function of temperature

Temperature (°C)	$\Delta\lambda_{max}$ (nm)[a]
18	2
22	7
26	4
30	6
35	6
40	7

[a] $\Delta\lambda_{max}$ (nm) indicates the shift of the emission maximum toward shorter wavelengths.

The long peptide, E2 (35–53) behaves similarly with DMPC vesicles: Trp λ_{max} does not change in presence of liposomes. Fig. 3a illustrates the Trp spectra at 18 and 40 °C, below and above, respectively DPPC main transition temperature (intermediate temperatures have been omitted for clarity). At 18 °C the two spectra superpose indicating a lack of interaction in the gel state, while at 40 °C Trp fluorescence intensity is slightly higher in presence of fluid SUVs. Finally, Fig. 3b shows the results after peptide titration with DMPG SUVs. There is a clear blue shift of λ_{max} (Table 4) both under and above Tm suggesting that the peptide changes its partitioning between the bilayer and the external polar medium. This effect seems to be independent of the rigidity of the bilayer for what we could suggest an interfacial interaction between the polar head of the phospholipid and the peptide. This was confirmed by the results described in Section 3.3. Finally, the ratio F/F_0 shows a different trend depending on the lipid. As seen in Fig. 2, F/F_0 at 18 °C is practically identical for DMPC and DMPG but it tends to increase with temperature for the anionic vesicles (DMPG). In presence of zwitterionic vesicles (DMPC) F/F_0 decreases in the vicinity of Tm afterwards it remains almost constant. The slight change in F/F_0 and the no modification on emission λ_{max} in presence of DMPC vesicles

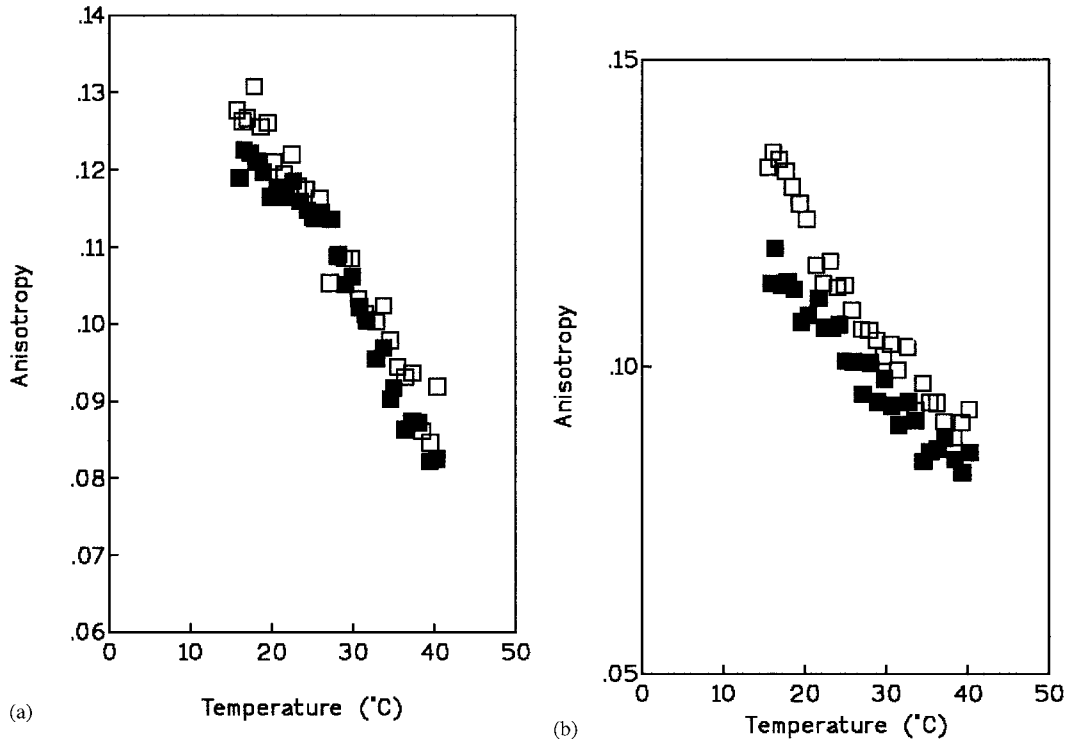

Fig. 4. Temperature dependence of the steady-state fluorescence anisotropy of NBD-PE labeled SUVs of: (a) DMPC; or (b) DMPG. Closed symbol: control; empty symbol: SUVs titrated with. 1.26 mM E2 (39–53). Lipid/peptide ratio into the cuvette: 100:4.

clearly indicates a lack of interaction between the long peptide and zwitterionic vesicles. Thus also the charge seems to play a role on peptide/lipid interaction. The same kind of interaction has been described for other fusogenic, acylated and cationic peptides [15,16].

3.3. Steady state fluorescence studies

We have used two probes that locate at different position in the bilayer to analyze the depth of peptide penetration into the membrane. TMA-DPH is anchored at the water/lipid interface with the hydrophobic fraction, DPH oriented parallel to the lipid fatty acid chains and the trimethylamonium group located close to the lipid headgroup. On another hand, NBD-PE tend, to sense the lipid–water interface region of membranes instead of the hydrophobic interior, therefore it is an indicator of the mobility of the headgroup region of the membranes.

The probe that reports on the anisotropy closest to the glycerol backbone region (TMA-DPH) did not show any change in chain mobility both in the DMPC or DMPG SUVs (fig not shown) in presence of any of the peptides. This indicates that the peptides had no effect in this region of the membrane. In the case of NBD-PE labeled SUVs, peptide as well as phospholipid composition was determinant critical in the anisotropy values. The 15-mer peptide did not change the anisotropy of any of the controls while the 22-mer peptide showed a different behaviour depending on the lipid.

Fig. 4a shows the heating curves of SUVs with and without E2 (39–53) incubated with NBD-PE labeled DMPC SUVs. Although changes are not important, peptide addition seems to play a weak rigidifying effect in the gel state ($r \sim 0.28$) if compared to the control ($r \sim 0.22$). Curve shapes superimpose at higher temperature thus indicating no effect in the fluid state. On another hand, E2 (39–53) decreased the mobility at the headgroup region for DMPG-SUVs, both below and above the Tm (23 °C), as seen by the increase of the anisotropy of the NBD-PE groups (Fig. 4b). Results suggest a surface interaction between the E2 (35–53) peptide and DMPG vesicles having thus peptide length as well as charge a role on membrane structure. Further studies are being performed to get insight on peptide structure influence on lipid mono and bilayers.

Acknowledgements

We gratefully acknowledge Helena Carvajal Laiglesia for excellent technical assistance. This work was supported by a grant BQU 2000/0793/CO2/01 from CICYT Spain.

References

[1] E.I. Pécheur, J. Sainte-Maire, A. Bienvenüe, D. Hoekstra, Membr. Biol. 167 (1999) 1.
[2] M. Magzoub, L.E.G. Eriksson, A. Gräslund, Biochim. Biophys. Acta 1563 (2002) 53.
[3] D. Derossi, S. Calvet, A. Trembleau, A. Bruinissen, G. Chassaing, A. Prochiantz, J. Biol. Chem. 271 (2001) 18 188.
[4] K. Lugardon, S. Chasserot-Golaz, A.E. Kieffer, R. Maget-Dana, G. Nullans, B. Kieffer, D. Aunis, J. Biol. Chem. 276 (2001) 35 875.
[5] I. Haro, A. Bosch, F. Reig, Curr. Top. Peptide Prot. Res. 1 (1994) 135.
[6] E. Pierschbacher, E. Ruoslahti, Nature 309 (1984) 30.
[7] P. Sospedra, C. Mestres, I. Haro, M. Muñoz, M.A. Busquets, Langmuir 18 (2002) 1231.
[8] K. Takahashi, M. Hijikata, K. Aoyama, H. Hoshino, K. Hino, S. Mishiro, Int. Hepatol. Commun. 6 (1997) 253.
[9] J.A. Pérez, J.F. González-Dankaart, F. Reig, R.M. Pintó, A. Bosch, I. Haro, Biomed. Peptides Proteins Nucleic Acids 1 (1995) 93.
[10] M.J. Gómara, V. Girona, G. Ercilla, F. Reig, M.A. Alsina, I. Haro, Biopolymers 58 (2001) 117.
[11] E. Kaiser, R.L. Colescott, C.D. Bossinger, P.I. Cook, Anal. Biochem. 34 (1970) 595.
[12] R. Verger, G.H. de Haas, Chem. Phys. Lipids 10 (1973) 127.
[13] G. Rouser, S. Fleisher, A. Yamamoto, Lipids 5 (1970) 494.
[14] C.L. Bashford, B. Chance, J.C. Smith, T. Yoshida, Biophys. J. 25 (1979) 63.
[15] T.B. Pederson, M.C. Sabra, S. Frokjaer, O.G. Mouritsen, K. Jørgensen, Chem. Phys. Lipids 113 (2001) 83.
[16] E.I. Pécheur, J. Sainte-Maire, A. Bienvenüe, D. Hoekstra, Biochem. 38 (1999) 364.